ORIGINAL ARTICLE

NbPTR1 confers resistance against *Pseudomonas syringae pv. actinidiae* in kiwifruit

Shin-Mei Yeh[1] | Minsoo Yoon[2] | Sidney Scott[1] | Abhishek Chatterjee[1] |
Lauren M. Hemara[2,3] | Ronan K. Y. Chen[4] | Tianchi Wang[1] |
Kerry Templeton[5] | Erik H. A. Rikkerink[2] | Jay Jayaraman[2] | Cyril Brendolise[1]

[1]New Cultivar Innovation, The New Zealand Institute for Plant & Food Research Limited (PFR), Mt Albert Research Centre, Auckland, New Zealand

[2]Bioprotection, The New Zealand Institute for Plant & Food Research Limited (PFR), Mt Albert Research Centre, Auckland, New Zealand

[3]School of Biological Sciences, University of Auckland, Auckland, New Zealand

[4]Food Innovation, The New Zealand Institute for Plant and Food Research Limited (PFR), Palmerston North, New Zealand

[5]New Cultivar Innovation, The New Zealand Institute for Plant and Food Research Limited (PFR), Motueka, New Zealand

Correspondence
Jay Jayaraman and Cyril Brendolise, The New Zealand Institute for Plant & Food Research Limited (PFR), Mt Albert Research Centre, Auckland 1025, New Zealand.
Email: Jay.Jayaraman@plantandfood.co.nz and cbrendo009@yahoo.fr

Funding information
New Zealand Institute for Plant and Food Research Limited

Abstract

Pseudomonas syringae pv. actinidiae biovar 3 (Psa3) causes a devastating canker disease in yellow-fleshed kiwifruit (*Actinidia chinensis*). The effector HopZ5, which is present in all isolates of Psa3 causing global outbreaks of pandemic kiwifruit canker disease, triggers immunity in *Nicotiana benthamiana* and is not recognised in susceptible *A. chinensis* cultivars. In a search for *N. benthamiana* nonhost resistance genes against HopZ5, we found that the nucleotide-binding leucine-rich repeat receptor NbPTR1 recognised HopZ5. RPM1-interacting protein 4 orthologues from *N. benthamiana* and *A. chinensis* formed a complex with NbPTR1 and HopZ5 activity was able to disrupt this interaction. No functional orthologues of NbPTR1 were found in *A. chinensis*. Nb*PTR1* transformed into Psa3-susceptible *A. chinensis* var. *chinensis* 'Hort16A' plants introduced HopZ5-specific resistance against Psa3. Altogether, this study suggested that expressing NbPTR1 in Psa3-susceptible kiwifruit is a viable approach to acquiring resistance to Psa3 and it provides valuable information for engineering resistance in otherwise susceptible kiwifruit genotypes.

KEYWORDS

Actinidia chinensis, effector-triggered immunity, HopZ5, *Nicotiana benthamiana*, Psa3, RNAi hairpin library

1 | INTRODUCTION

Pseudomonas syringae pv. *actinidiae* (Psa) is a bacterial plant pathogen which causes a devastating canker disease in kiwifruit. Symptoms of Psa infection include blossom necrosis, cane dieback, trunk/cane bleeding, cankerous growths and necrotic leaf spots (Scortichini et al., 2012). Psa was first isolated in Japan (in the 1980s) with subsequent outbreaks reported throughout China, Korea, Italy and

New Zealand (Kim et al., 2017; Scortichini, 1994; Serizawa et al., 1989; Vanneste, 2017). Since 2008, the emergence of a highly virulent lineage of Psa biovar 3 (Psa3; also called the pandemic lineage of Psa3) has led to significant losses in kiwifruit production worldwide. This pandemic lineage is particularly virulent towards yellow-fleshed kiwifruit (*Actinidia chinensis*), which is a major crop for both Italy and New Zealand (Scortichini, 1994; Vanneste, 2017). Currently, Psa's impact is mainly mitigated through hygienic orchard practices.

However, the development of a more tolerant cultivar has played a key role in the short to medium-term management of the disease. Achieving robust Psa resistance has however become an important longer-term target of kiwifruit breeding programmes.

Plants have evolved two key modes of defence against invading pathogens such as Psa. The first is pattern-triggered immunity (PTI), which relies upon the recognition of pathogen-associated molecular patterns (PAMPs) by specific pattern-recognition receptors (PRRs) at the plant cell surface (Jones & Dangl, 2006). Pathogenic bacteria have in turn developed the ability to overcome PTI by injecting host cells with virulence proteins called effectors. Effectors are delivered into host cells through a type III secretion system (T3SS) and can facilitate infection by interfering with pattern recognition and allowing pathogens to evade immune detection (Alfano et al., 2000). To counteract effectors, plants have developed a second layer of defence called effector-triggered immunity (ETI), which involves intracellular receptors to recognise bacterial effectors and triggers the immune response. ETI produces a robust immune response by restoring and potentiating PTI (Ngou et al., 2021). ETI often results in a form of programmed cell death known as the hypersensitive response (HR), which allows plants to kill off infected cells to prevent further disease spread (Cui et al., 2015; Dangl & Jones, 2001).

ETI is governed by the aforementioned intracellular, nucleotide-binding domain, leucine-rich repeat receptors commonly referred to as NLRs (Dangl & Jones, 2001). NLRs can sense effectors that are secreted by pathogens into plant cells by a variety of mechanisms, including a type III secretion system (T3SS) carried by some bacterial pathogens like Psa. Effectors translocated into plant cells via the T3SS are known as type III effectors (T3Es) (Block et al., 2008) and are commonly named Hop (Hrp outer protein) or Avr (avirulence) proteins (Lindeberg et al., 2012). Psa3 carries approximately 39 T3Es, including two effectors (HopZ5 and HopH1) that are unique to this highly virulent biovar (McCann et al., 2013). Several *P. syringae* T3E proteins target host RPM1-INTERACTING PROTEIN 4 (RIN4) but trigger ETI owing to the NLRs guarding RIN4 (Kim et al., 2023). The *P. syringae* pv. *tomato* effector AvrRpt2 cleaves RIN4 to generate a product involved in activating RPS2-mediated immunity in *Arabidopsis thaliana* (Axtell & Staskawicz, 2003; Mackey et al., 2003). Similar RIN4 cleavage mechanisms have been found for Mr5-mediated defence responses in apple (Fahrentrapp et al., 2013) and Ptr1-mediated recognition of AvrRpt2 in tomato (Mazo-Molina et al., 2019). In soybean, RIN4 modification is involved in the recognition of AvrB and AvrRpm1 by Rpg1b and Rpg1r, respectively (Kessens et al., 2014). Recently, Jayaraman et al. (2023) found that five pathogenicity-associated Psa biovar 3 effectors (HopZ5a, HopH1a, AvrPto1b, AvrRpm1a and HopF1e) are collectively essential for full Psa3 virulence and that they largely target host RIN4 proteins. Although most Psa T3Es have been identified, we have yet to fully uncover which NLR proteins are responsible for recognizing and responding to specific effectors during ETI. Previously, Brendolise et al. (2017) constructed a hairpin-RNAi library targeting 345 NLR gene candidates identified in *Nicotiana benthamiana* (Brendolise et al., 2017). This library has been used to identify several NLR

genes that are able to recognize effectors from Psa. For example, NRG1 (N requirement gene 1) and RPA1 (Resistance to *Pseudomonas syringae* pv. *actinidiae* 1) have been shown to be involved in the recognition of Psa effectors HopQ1 and AvrRpm1, respectively (Brendolise et al., 2018; Yoon & Rikkerink, 2020).

The Psa effector HopZ5 is a member of the *Yersinia* outer protein J (YopJ) effector family and has an acetyltransferase activity that triggers HR in *A. thaliana* and *N. benthamiana* (Choi et al., 2017; Jayaraman et al., 2017). Several R genes have been shown to mediate HopZ5-triggered immunity in these model species. *RPM1* (RESIST-ANCE TO *P. SYRINGAE* PV. *MACULICOLA* 1) is required for HopZ5-triggered immunity in *Arabidopsis*, responding to HopZ5's acetylation of threonine residue T166 of AtRIN4 (Choi et al., 2021). In *N. benthamiana*, HopZ5 recognition depends on several NLR genes, depending on the genotype of *N. benthamiana* used: *PTR1* (PSEU-DOMONAS TOMATO RACE 1) and *ZAR1* (HOPZ-ACTIVATED RESIST-ANCE 1), with the assistance of *JIM2* (XOPJ4 IMMUNITY 2) for the latter in Nb-0, and only *PTR1* in Nb-1 plants (Schultink et al., 2019). The evaluation of a set of Psa3 effector knockouts suggests that HopZ5 is not recognised in susceptible *A. chinensis* (Hemara et al., 2022). Hence, we hypothesized that introducing HopZ5-recognizing *R* genes into *A. chinensis* could be a promising approach for facilitating ETI and improving resistance to Psa. This study demonstrates the independent identification of *PTR1a* as an NLR which recognizes HopZ5 in *N. benthamiana*, as well as the transformation of Nb*PTR1a* into previously susceptible *A. chinensis*. We show that Nb*PTR1a*-expressing *A. chinensis* var. *chinensis* 'Hort16A' plants display significantly improved resistance to Psa3 via reduced *in planta* bacterial growth and disease symptoms, owing to a specific HopZ5-triggered resistance response.

2 | RESULTS

2.1 | NbPTR1a mediates HopZ5-triggered immunity in *N. benthamiana*

Previous studies have demonstrated that HopZ5 triggers a significant HR in *Nicotiana* spp. (Choi et al., 2017). To identify the NLR gene(s) responsible for mediating HopZ5 recognition in *N. benthamiana*, HopZ5 was screened against a library of NLR gene-silencing RNA interference (RNAi) hairpin constructs following the methodology previously described (Brendolise et al., 2017). One hairpin construct (hp#1) was shown through transient expression assays to interfere with HopZ5-triggered HR (Figure 1a). hp#1 contains six DNA fragments, each targeting different NLR genes (with some occasional overlap): m1, m2, u10, u120, u147 and u156 (Brendolise et al., 2017). To identify the fragment responsible for interfering with HopZ5-triggered HR, each hairpin fragment was individually sub-cloned and screened. Only fragment m1 was able to reduce the HopZ5-triggered HR (Figure 1b). m1 targets two genes within the *N. benthamiana* genome (Bombarely et al., 2012): Nb*PTR1a* (NbS00012936g0019.1) and Nb*PTR1b* (NbS00007796g0005.1) (Figure 1c). Nb*PTR1b* is

rendered nonfunctional owing to the presence of a premature stop codon (Mazo-Molina et al., 2020), suggesting that Nb*PTR1a* is likely to encode the NLR required for this immune response.

To confirm that Nb*PTR1a* is required for HopZ5-triggered immunity, endogenous Nb*PTR1a* was silenced and complemented with a synthetic analogue Nb*PTR1syn*. NbPTR1syn amino acid sequence is identical to NbPTR1a but has a modified nucleotide sequence to elude silencing by the m1 hairpin construct (Figure S1). Transient coexpression of Nb*PTR1syn* with HopZ5 was able to restore HR to the Nb*PTR1a*-silenced leaf patches, supporting the idea that functional Nb*PTR1a* is required for the recognition of HopZ5 (Figure 1d). HR was also quantified by measuring the conductivity due to ion leakage from the corresponding infiltrated patches. Coexpression of m1 and Nb*PTR1syn* in the presence of HopZ5 showed a significant restoration of ion leakage (Figure 1e). These results indicated that Nb*PTR1a* could recognize HopZ5 to trigger HR in *N. benthamiana*, consistent with previous observations (Ahn et al., 2023).

While HopZ5-triggered HR was reduced by m1 expression in the transient assay, ion leakage was only partially reduced (Figure 1e). Ahn et al. (2023) found that Nb*ZAR1* was also involved in the recognition of HopZ5 in *N. benthamiana*. Therefore, we identified two silencing fragments from our hairpin library, m16 and u38, which correspond to the nucleotide-binding-ARC (NB-ARC) domain or the coiled-coil (CC) domain of Nb*ZAR1*, respectively (Figure S2a). Neither silencing construct alone nor the combined m16/u38 constructs were able to block HopZ5-triggered HR to the extent that silencing Nb*PTR1a* could (Figures S2b and S2c). To check if silencing constructs were efficiently silencing their targets, endogenous Nb*PTR1* and Nb*ZAR1* expression was checked. RT-qPCR of Nb*PTR1* and Nb*ZAR1* showed that Nb*PTR1* expression is reduced by *PTR1*-targeting m1 but not with *ZAR1*-targeting m16/u38; whereas Nb*ZAR1* expression is reduced with m16/u38 but not with m1, as expected (Figure S2d). These collective results did not identify Nb*ZAR1* as a significant contributor to HopZ5-triggered HR under these experimental conditions.

2.2 | RIN4 is involved in the recognition of HopZ5 in *N. benthamiana*

Yoon and Rikkerink (2020) previously cloned multiple *RIN4* orthologues from *N. benthamiana* (NbRIN4-1: Nbv6.1trP32525, NbRIN4-2: Nbv6.1trP59092 and NbRIN4-3: Niben101Scf03488g06005) and *A. chinensis* var. *chinensis* 'Hort16A' (AcRIN4-1, AcRIN4-2 and AcRIN4-3) (Figure S3a). Physical association of NbPTR1a with these RIN4 orthologues were tested by co-immunoprecipitation (co-IP). Interestingly, of the three NbRIN4 orthologues, only NbRIN4-1 was able to interact stably with NbPTR1a (Figure S3b). We tested the ability of NbPTR1a to interact with three kiwifruit RIN4 homologues (Figure 2a). Notably, only AcRIN4-2 showed strong physical interactions with NbPTR1a, while a weak or no interaction was found with AcRIN4-1 and AcRIN4-3, respectively. Recently, Jayaraman et al. (2023) found that

HopZ5 interacted with AcRIN4-1 and AcRIN4-2 and weakly with AcRIN4-3 *in planta*. To determine the potential association between HopZ5 and NbPTR1a with a bridging interaction by AcRIN4-2, we performed a three-component coimmunoprecipitation experiment with coexpression of NbPTR1a:Myc, HopZ5:YFP and FLAG:AcRIN4-2 (Figure 2b). Surprisingly, we found that when NbPTR1a was immunoprecipitated in the presence of AcRIN4-2, HopZ5 was not coprecipitated. These results suggested either, that despite strongly interacting with HopZ5 and NbPTR1a, AcRIN4-2 does not bridge the HopZ5-PTR1a interaction, or that HopZ5 modifies AcRIN4-2 in a way that eliminates interaction with NbPTR1a. To assess this possibility, AcRIN4-2 was checked for interaction with NbPTR1a, in the presence of HopZ5, HopZ5C218A catalytic dead mutant (Jayaraman et al., 2017), or in the absence of HopZ5 (Figure 2c). Notably, only the presence of enzymatically active HopZ5 abolished the ability of AcRIN4-2 to interact with NbPTR1a, probably allowing NbPTR1a to trigger immunity as a consequence.

To investigate this interaction model further, we used Alpha-Fold2 multimer implemented in Colabfold (Mirdita et al., 2022) to assess the likelihood of direct interaction between the six RIN4 proteins (three RIN4 homologues from *N. benthamiana* and three from *A. chinensis*) and NbPTR1a. Two well understood RIN4-R protein systems from *Arabidopsis* (AtRIN4 interacting with AtRPM1 or AtRPS2) and another *Arabidopsis* NLR protein interacting with its well-structured guardee protein (AtPBS1 interacting with AtRPS5) were used as controls. The resulting very poor pDockQ scores (Table S1) imply that direct interaction between RIN4s and NbPTR1a is unlikely to be the basis of this resistance-triggering system. Interestingly, the ipTM:pTM and pDockQ scores for the two other well-known interacting NLRs with AtRIN4 (AtRPM1 and AtRPS2) are similarly low whereas the score for the well-known structured kinase interacting model (AtPBS1 with AtRPS5) has significantly better ipTM:pTM and pDockQ scores in the acceptable range.

To confirm the in silico modelling results, Nb*PTR1a*, *hopZ5*, Nb*RIN4*s and Ac*RIN4*s were cloned into yeast vectors and direct interactions assessed for NbPTR1a with NbRIN4s and AcRIN4s as well as HopZ5 and AcRIN4s. These interactions were tested in both directions as bait and prey, with consistent results; a representative interaction data set is presented here (Figure S4). As predicted by the modelling, none of the RIN4s were able to interact directly with NbPTR1a. Notably, despite being shown to interact with HopZ5 in planta previously (Jayaraman et al., 2023), AcRIN4s also did not interact with HopZ5 directly in this in vitro assay.

2.3 | AcPTR1 homologues could not complement loss of NbPTR1a in *N. benthamiana*

Most *A. chinensis* var. *chinensis* varieties are unable to mount a defence response to Psa3 carrying HopZ5 (Hemara et al., 2022; Jayaraman et al., 2023). This may be due to the lack of a suitable R gene or the lack of a guardee. To assess if any functional homologues (orthologues) of Nb*PTR1a* were present in
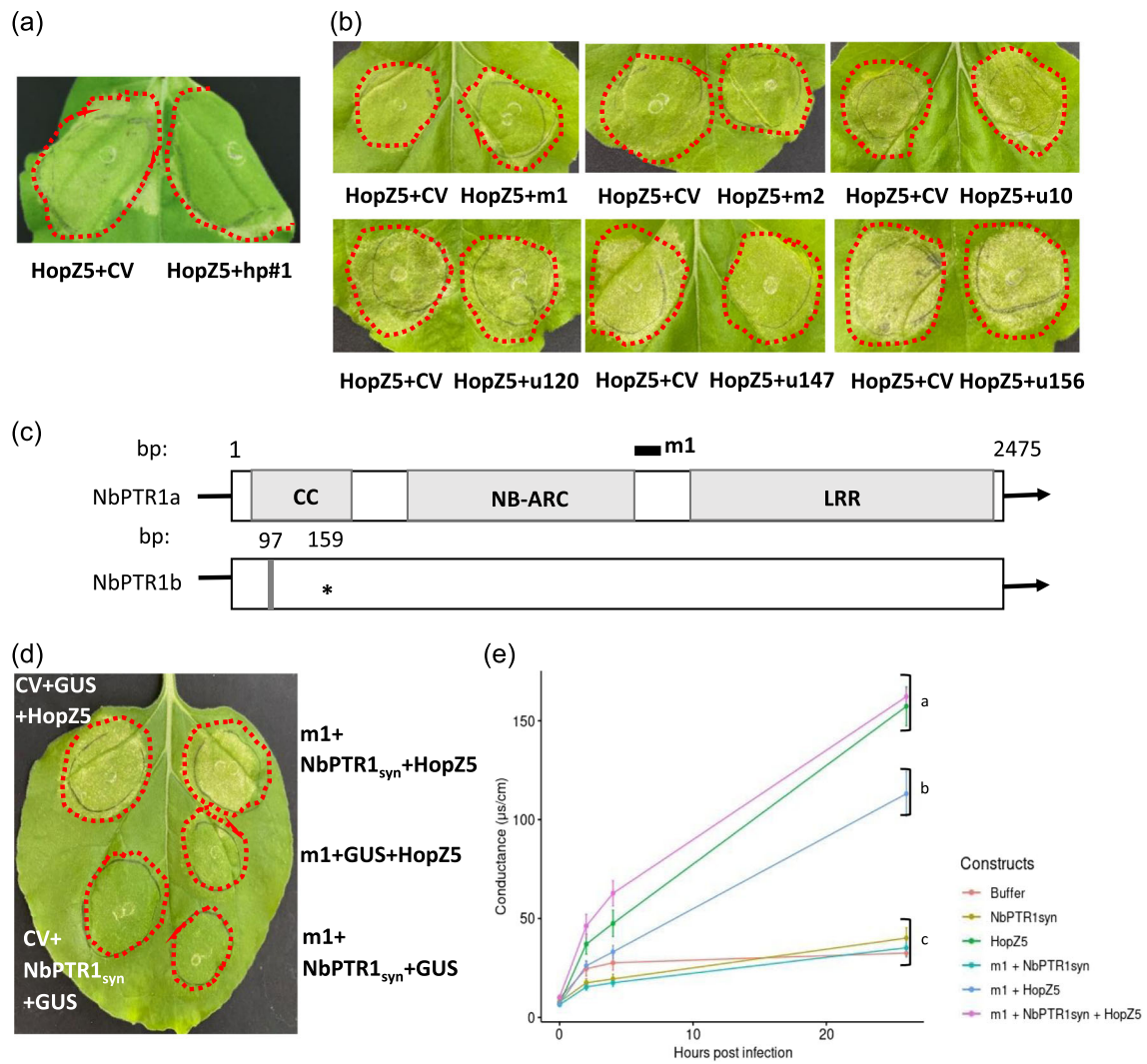
FIGURE 1 NbPTR1a mediates a HopZ5-triggered immune response in *Nicotiana benthamiana*. (a, b) HopZ5-triggered hypersensitive response (HR) is reduced by hp#1 and the m1 fragment. *N. benthamiana* leaves were agroinfiltrated with pTKO2_GGT control vector (CV), hp#1, or one of six DNA target fragments in hp#1: m1, m2, u10, u120, u147 and u156, each at OD_{600} of 0.2, followed by agroinfiltration of HopZ5 (OD_{600} of 0.05) 48 h later. Leaves were photographed 6 days postinoculation (dpi). Red dash line indicated the HopZ5-inoculated area. (c) Schematic of PTR1 gene structure in *N. benthamiana* (Nb*PTR1a* and Nb*PTR1b*). The coiled-coil (CC), nucleotide binding site present in APAF-1, R proteins and CED-4 (NB-ARC), and leucine-rich repeat (LRR) domains are indicated in grey rectangles. The black bar indicates the area targeted by m1, corresponding to position 1291–1441 bp relative to Nb*PTR1a*. Nb*PTR1b* has a 5-bp deletion (grey bar) at position 97 bp resulting in a premature stop codon (asterisk) at position 159 bp. (d) Transient complementation of NbPTR1syn. *N. benthamiana* leaves were agroinfiltrated with m1 + NbPTR1syn, m1 + GUS, CV + NbPTR1syn or CV + GUS, each at OD_{600} of 0.1, followed by agroinfiltration with HopZ5 or GUS control (each at OD_{600} of 0.2) 48 h later. Leaves were photographed 4 dpi. (e) Quantification of the HR by electrolyte leakage. Conductivity was measured from leaf disks collected at 2 day postfinal infiltration from the leaf patches shown in (d). Error bars represent the standard errors of the means for 10 independent biological replicates, collected from two independent experimental runs ($n = 10$). HopZ5 was used as positive control and infiltration buffer (10 mM $MgCl_2$, 100 µM acetosyringone) as a negative control. Letters indicate statistically significant differences from a one-way analysis of variance and Tukey's HSD post hoc test for values at 26 h postsampling.

Psa3-susceptible *A. chinensis* var. *chinensis*, the published 'Red5' genome was searched for Nb*PTR1a* homologues (Pilkington et al., 2018). Two kiwifruit *PTR1a* homologues were identified in 'Red5' and genes amplified from *A. chinensis* var. *chinensis* 'Hort16A' genomic DNA. Both alleles for each gene were cloned: Ac*PTR1a*-1, Ac*PTR1a*-2, Ac*PTR1b*-1 and Ac*PTR1b*-2 (Figure S5). The nucleotide sequence of Nb*PTR1a* is 55% and 56% identical to those of

Ac*PTR1a* and Ac*PTR1b*, respectively. To confirm whether the four Ac*PTR1*s were the closest kiwifruit homologues of Nb*PTR1a*, a reciprocal BLAST search was conducted for each of the Ac*PTR1* homologues' NB-ARC domains against the *N. benthamiana* genome. Four gene candidates were identified: NbS00012936 (Nb*PTR1a*), NbS00007796 (Nb*PTR1b*), NbS00034734 and NbS00047736. A phylogenetic analysis of the NB-ARC domain of the *N. benthamiana*
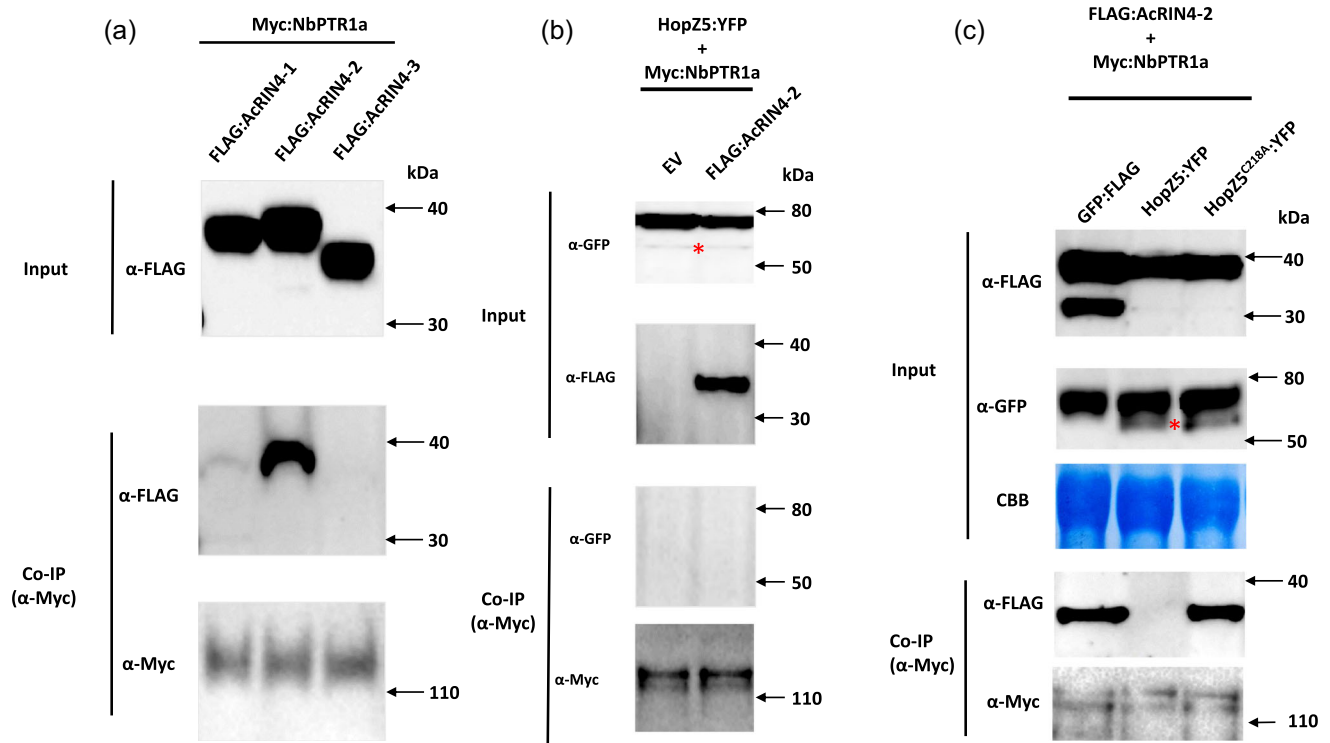
FIGURE 2 AcRIN4-2 is involved in NbPTR1a-mediated recognition of HopZ5. (a) Coimmunoprecipitation of NbPTR1a and RIN4 homologues. NbPTR1a and RIN4 homologues were coexpressed simultaneously via agroinfiltration, each at OD_{600} of 0.1. 2 days postinfiltration, leaf samples were harvested, protein extracts prepared and precipitated using anti-Myc antibody. Western blot of input and precipitated proteins were probed with anti-FLAG or anti-Myc antibody. The experiments were conducted twice with similar results. (b) Coexpression of AcRIN4-2 with NbPTR1a does not facilitate HopZ5a immunoprecipitation with NbPTR1a. YFP-tagged HopZ5 (or YFP alone), Myc-tagged NbPTR1a, and FLAG-tagged AcRIN4-2 were expressed simultaneously by agroinfiltration, each at OD_{600} of 0.1. 2 days postinfiltration, leaf samples were harvested, and protein extracts prepared and precipitated using anti-Myc antibody. Western blots of input and precipitated proteins were probed with anti-GFP or anti-Myc antibody. IP, coimmunoprecipitation. (c) HopZ5 function abolishes coimmunoprecipitation of AcRIN4-2 with NbPTR1a. YFP-tagged HopZ5, HopZ5^{C218A} noncatalytic mutant, or FLAG control was expressed with Myc-tagged NbPTR1a and FLAG-tagged AcRIN4-2 simultaneously by agroinfiltration, each at OD_{600} of 0.1. 2 days postinfiltration, leaf samples were harvested, and protein extracts prepared and precipitated using anti-Myc antibody. Western blots of input and precipitated proteins were probed with anti-GFP, anti-FLAG, or anti-Myc antibody as indicated. CBB, coomassie brilliant blue; IP. The red asterisk in the input anti-GFP panels in (b) and (c) represent the expected band size for HopZ5:YFP. The western blot experiments were conducted at least three times with identical results. [Color figure can be viewed at wileyonlinelibrary.com]

candidates and Ac*PTR1* homologues showed that the four Ac*PTR1* homologues formed a single group phylogenetically closer to the clade with NbS00034734 and NbS00047736 than that of Nb*PTR1a* (Figure 3a). However, the lengths of the two *N. benthamiana* genes are much shorter than those of the Ac*PTR1* homologues or Nb*PTR1a*; NbS00034734 has a truncated NB-ARC domain and NbS00047736 lacks its LRR domain. Further searches of the Red5 genome did not identify any additional closer homologues of NbS00034734, and NbS00047736. This result suggested that, the identified Ac*PTR1a*/Ac*PTR1b* candidates are probably the closest functional NLRs present in 'Hort16A' to Nb*PTR1a* and its homologues.

Several RIN4-related NLR genes have been identified, including At*RPS2*, Md*Mr5*, Sl*Ptr1*, Gm*RPG1r*, Gm*RPG1b*, At*RPM1*, At*ZAR1* and Nb*ZAR1* (Ahn et al., 2023; Axtell & Staskawicz, 2003; Choi et al., 2021; Fahrentrapp et al., 2013; Kessens et al., 2014; Mazo-Molina et al., 2019). To understand the broader relationships of Ac*PTR1* candidates and AcPTR1 homologues with these NLR proteins involved in recognition of RIN4-associated effectors, the NB-ARC domains of each NLR protein were also included in our phylogenetic analysis (Figure 3a). This revealed that that there is strong support for the clade shared by Ac*PTR1* homologues and Nb*PTR1a*/Sl*Ptr1*, but weak support for exclusion of the clade with Gm*RPG1b*/Gm*RPG1r* and At*ZAR1*/Nb*ZAR1*, suggesting a RIN4-guarding function for the AcPTR1 homologues.

To assess whether the four identified kiwifruit *PTR1* homologues could recognise HopZ5 in *N. benthamiana*, endogenous Nb*PTR1a* was silenced by the m1 construct and complemented by each Ac*PTR1* homologue (Figure 3b). None of the Ac*PTR1* homologues was able to restore HopZ5-triggered HR. These results indicate that the four identified kiwifruit PTR1 homologues do not function like NbPTR1a to recognize HopZ5 in *N. benthamiana*, suggesting that no PTR1-like orthologue exists in 'Hort16A' plants, commensurate with their Psa3-susceptible status.
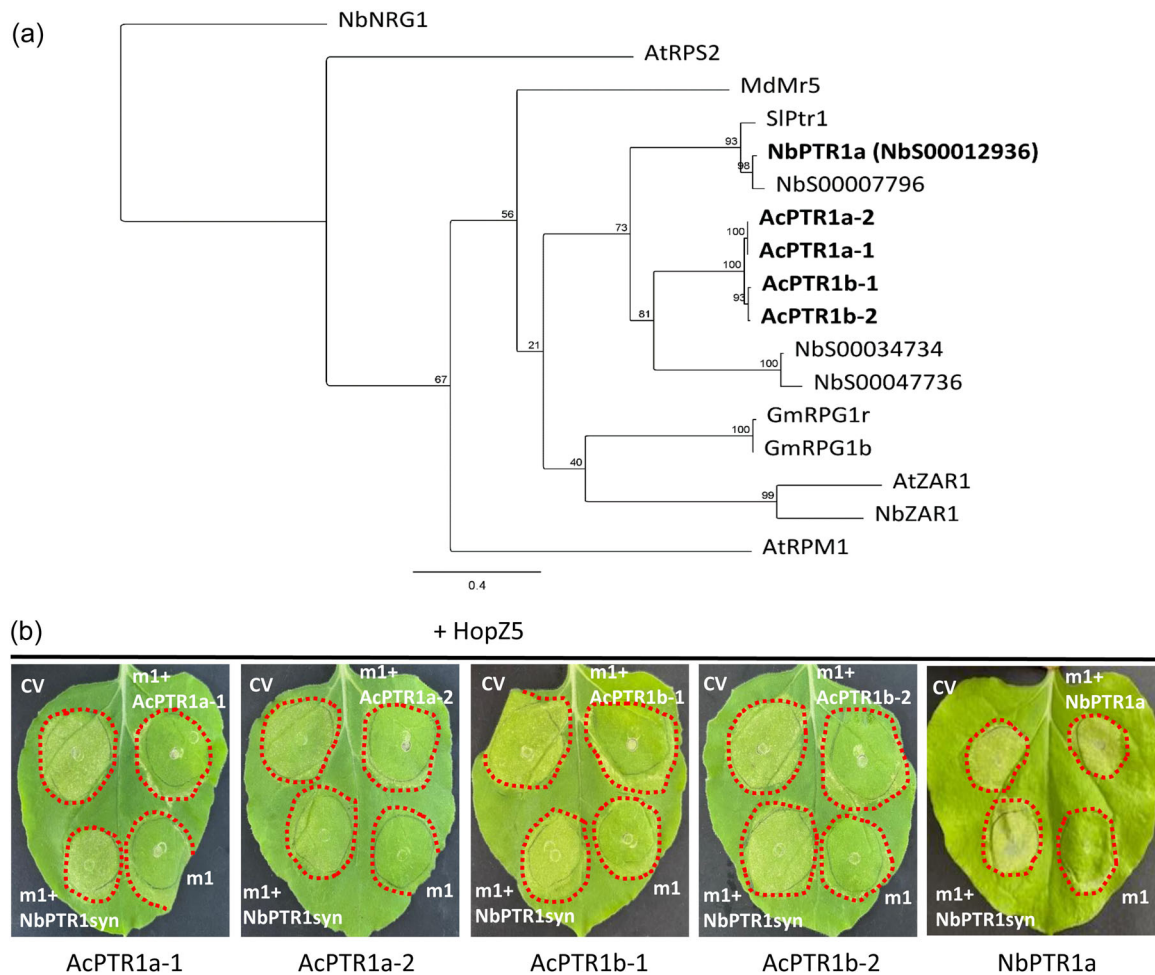
FIGURE 3 Ac*PTR1* homologues cannot complement silencing of Nb*PTR1a* in *Nicotiana benthamiana*. (a) Phylogenetic relationship of R genes involved in the recognition of RIN4-associated effectors including Ac*PTR1* homologues and their most closely related genes in *N. benthamiana*. Nucleotide sequences of NB-ARC domains were aligned by using MUSCLE alignment. The nucleotide distance was calculated by GTR GAMMA model and the tree was constructed by using RAxML with 100 bootstrap replicates in Geneious Prime. Sequences were sourced from *N. benthamiana* (Nb), *Solanum lycopersicoides* (Sl), *Arabidopsis thaliana* (At), *Actinidia chinensis* (Ac), *Glycine max* (Gm), or *Malus domestica* (Md). The tree was drawn to scale. Labels on branches indicate the percentage of bootstrap support with Nb*NRG1* used as outgroup. R genes of interest are indicated in bold font. (b) Transient complementation of kiwifruit *PTR1a* homologues. Four *PTR1a* homologues were identified in kiwifruit: Ac*PTR1a-1*, Ac*PTR1a-2*, Ac*PTR1b-1* and Ac*PTR1b-2*. *N. benthamiana* leaves were agroinfiltrated with the m1 hairpin construct and individual Ac*PTR1* homologues, as indicated, each at OD_{600} of 0.05, followed by agroinfiltration with HopZ5 (OD_{600} of 0.2) 48 h later. Leaves were photographed 4 dpi. Red dashed lines indicate the HopZ5-inoculated area. The experiments were performed in at least three independent leaves, across three independent experiments with similar results. CV, control vector. [Color figure can be viewed at wileyonlinelibrary.com]

2.4 | Overexpression of Nb*PTR1a* in kiwifruit confers resistance against Psa3 infection

Hemara et al. (2022) previously found that HopZ5 was not recognised in susceptible *A. chinensis* var. *chinensis* 'Hort16A' plants and did not trigger an HR. Both RPM1 and PTR1 play an important role in HopZ5-triggered immunity in *A. thaliana* and *N. benthamiana*, respectively (Ahn et al., 2023; Choi et al., 2021). This suggested that transformation of either At*RPM1* or Nb*PTR1* into kiwifruit might trigger recognition of HopZ5 and be associated with resistance to Psa3. Therefore, stable 'Hort16A' transformants expressing either At*RPM1* or Nb*PTR1a* under the control of a 35 S CaMV promoter were generated. The resulting transgenic plantlets (grown in axenic

tissue culture) were flood-inoculated with Psa3 ICMP 18884 (also called Psa3 V-13). Plantlets were monitored for development of classic bacterial canker symptoms over a 6-week period to assess resistance. Similarly to β-glucuronidase (GUS) control transgenic plants, most At*RPM1* transgenic plantlets did not survive for 6 weeks postinfection, whereas the majority of Nb*PTR1a* transgenic plantlets showed moderate to high survival under similar inoculation conditions (Table S2). These preliminary results suggested that the Nb*PTR1a* transgenic 'Hort16A' plants are more resistant to Psa3 than At*RPM1* transgenic 'Hort16A' plants.

Amongst the Nb*PTR1a* transgenic plants, Line 1A was consistently susceptible to Psa3 infection (Table S2). The level of expression of the Nb*PTR1a* transgene was quantified by qPCR and

revealed that the five selected NbPTR1a transgenic lines showed varied levels of NbPTR1a expression (Figure 4a). Interestingly, Line 1A showed a very low level of expression of the transgene, consistent with a lack of resistance to Psa3 measured in our preliminary experiments. Furthermore, we found no differences in the growth phenotypes between the NbPTR1a transgenic plants and wild-type Hort16A plants. To further assess the resistance to Psa3 of the NbPTR1a transgenic plants, an *in planta* bacterial growth assay was conducted on mature glasshouse plants. Fully expanded leaves were inoculated and Psa3 growth was quantified at 7 days postinoculation (dpi) by PDQeX-qPCR (Figure 4b). At 7 dpi the four moderate-to-high expressing lines (4, 7D, 13A, and 14) significantly restricted *in planta* Psa3 growth, whereas the very low expressing Line 1A showed no significant difference from wild-type 'Hort16A' or GUS control plants. These results showed that the expression of the NbPTR1a transgene conferred resistance to Psa3 in 'Hort16A' in both immature tissue culture and mature glasshouse-grown plants.

To further confirm that NbPTR1a-mediated growth restriction was specifically related to the recognition of HopZ5, the five selected transgenic lines were grown in tissue culture and flood-inoculated with wild-type Psa3 or Psa3 ΔhopZ5, a Psa3 strain mutated to lack the *hopZ5* effector gene (Hemara et al., 2022). The disease phenotypes from flood-inoculated plantlets were assessed for up to 6 weeks postinoculation. The disease symptoms included necrosis/ leaf wilting, leaf spots, and white spots with numerical categories assigned (Figures 5a and S6a). Disease phenotypes were quantified using an adapted 'area under the disease progression curve' (AUDPC) methodology (Figures S6b and S6c) (Schandry, 2017). The disease

symptomology indicated that the four NbPTR1a moderate-to-high expressing lines (4, 7D, 13A and 14) showed a significant decrease in symptom development over the 6 weeks when inoculated with Psa3, whereas no difference in symptom development for these lines was observed in comparison to the GUS control and low expression Line 1A plants when plantlets were inoculated with Psa3 ΔhopZ5 (Figure 5b). Next, the plantlets were inoculated under the same conditions with Psa3 or Psa3 ΔhopZ5 strains and the *in planta* bacterial growth was quantified at 10 dpi by PDQeX-qPCR (Figure 5c). Similarly to the disease progression results, *in planta* growth of Psa3 was greatly restricted in the four moderate-to-high expressing lines (4, 7D, 13A, and 14) compared with the GUS control and low-expressing Line 1A plantlets. No similar growth restriction was measured with the Psa3 ΔhopZ5 strain, suggesting that Psa3 growth restriction is specifically due to HopZ5 recognition. Additionally, the disease symptomology and *in planta* growth assays of the tissue culture-grown NbPTR1a plantlets reflected closely the results obtained previously with the glasshouse-grown plants.

To assess whether the NbPTR1a transgenic plants could specifically recognize HopZ5 activity to trigger resistance to Psa3, a biolistic transformation reporter eclipse assay was conducted on tissue culture plantlet leaves as previously described by Jayaraman et al. (2021). A GUS reporter gene was coexpressed together with either HopZ5 or its nonfunctional HopZ5-C218A mutant by DNA bombardment in the leaves of the transgenic lines (Figure 5d). The effector HopA1 from *P. syringae* pv. *syringae* 61 was used as a positive control for HR in this assay (Jayaraman et al., 2021). Three transgenic lines (4, 7D, and 13A) showed significant reduction in GUS
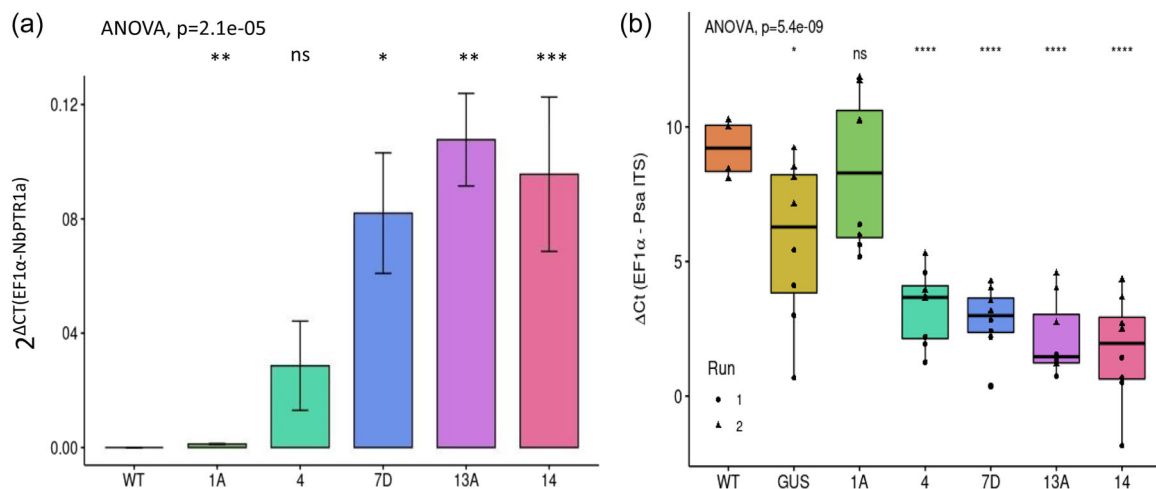
FIGURE 4 NbPTR1a transgenic kiwifruit plants are resistant to Psa3. (a) Quantitative polymerase chain reaction quantification of *PTR1* expression in five selected NbPTR1a transgenic lines. The NbPTR1a transgene expression is normalised to reference gene, AcEF1α. Wild-type Hort16A plants were used as a negative control. Data were shown as means ± SEM of three biological replicates. Asterisks indicate results of a one-way analysis of variance (ANOVA) and a two-tailed Welch's post hoc *t*-test between the selected transgenic lines and wild-type Hort16A; *$p < 0.05$, **$p < 0.01$, ***$p < 0.001$, and ns, nonsignificant. (b) Bacterial growth quantification in NbPTR1a transgenic glasshouse-grown plants. Leaves were inoculated with Psa3 at approximately 10^7 CFU/mL and bacterial growth was determined at 7 days postinfection (dpi). Wild-type Hort16A and β-glucuronidase (GUS) transgenic lines were used as negative controls. Error bars represent standard error of the mean from four biological replicates. Asterisks indicate results of a one-way analysis of variance and a two-tailed Welch's post hoc *t*-test between the selected transgenic lines and wild-type Hort16A; *$p < 0.05$, **$p < 0.01$, ***$p < 0.001$, ****$p < 0.0001$, and ns, nonsignificant. [Color figure can be viewed at wileyonlinelibrary.com]

activity when cobombarded with HopZ5 but not with the enzymatically dead HopZ5-C218A in comparison to the GUS bombardment alone. These results indicated that NbPTR1a transgenic plants could specifically recognize HopZ5 acetyltransferase activity to trigger an HR. There was a small, nonsignificant decrease in GUS activity visible when comparing GUS bombardment alone with HopZ5 for Line 14 but this was surprisingly no different from the response to HopZ5-C218A.

To confirm that NbPTR1a mediates the recognition of HopZ5 in transgenic plants, transgenic glasshouse plant leaves were vacuum-infiltrated with Psa3, Psa3 ΔhopZ5, or Psa3 ΔhrcC, and HR was evaluated by ion leakage measurement (Figure S7). The Psa3 ΔhrcC

strain was used as a negative control for HR in this assay owing to its lack of a type III secretion system and an associated inability to cause an effector-triggered HR. Surprisingly, no significant difference for HR-associated ion leakage was visible in these NbPTR1a transgenic plants when inoculated with Psa3 or Psa3 ΔhopZ5, similar to that observed in GUS control plants. Psa3 ΔhrcC showed low leakage as expected owing to its inability to secrete effectors. Due to the ability of Psa3 to suppress effector-triggered HR likely though effector-effector interference (Jayaraman et al., 2021), *P. fluorescens* PF0-1 artificially carrying the type III secretion system from *P. syringae* pv. *syringae*, called Pfo(T3S) (Thomas et al., 2009) was used to deliver HopZ5 into the transgenic NbPTR1 and GUS plants (Figure S8).
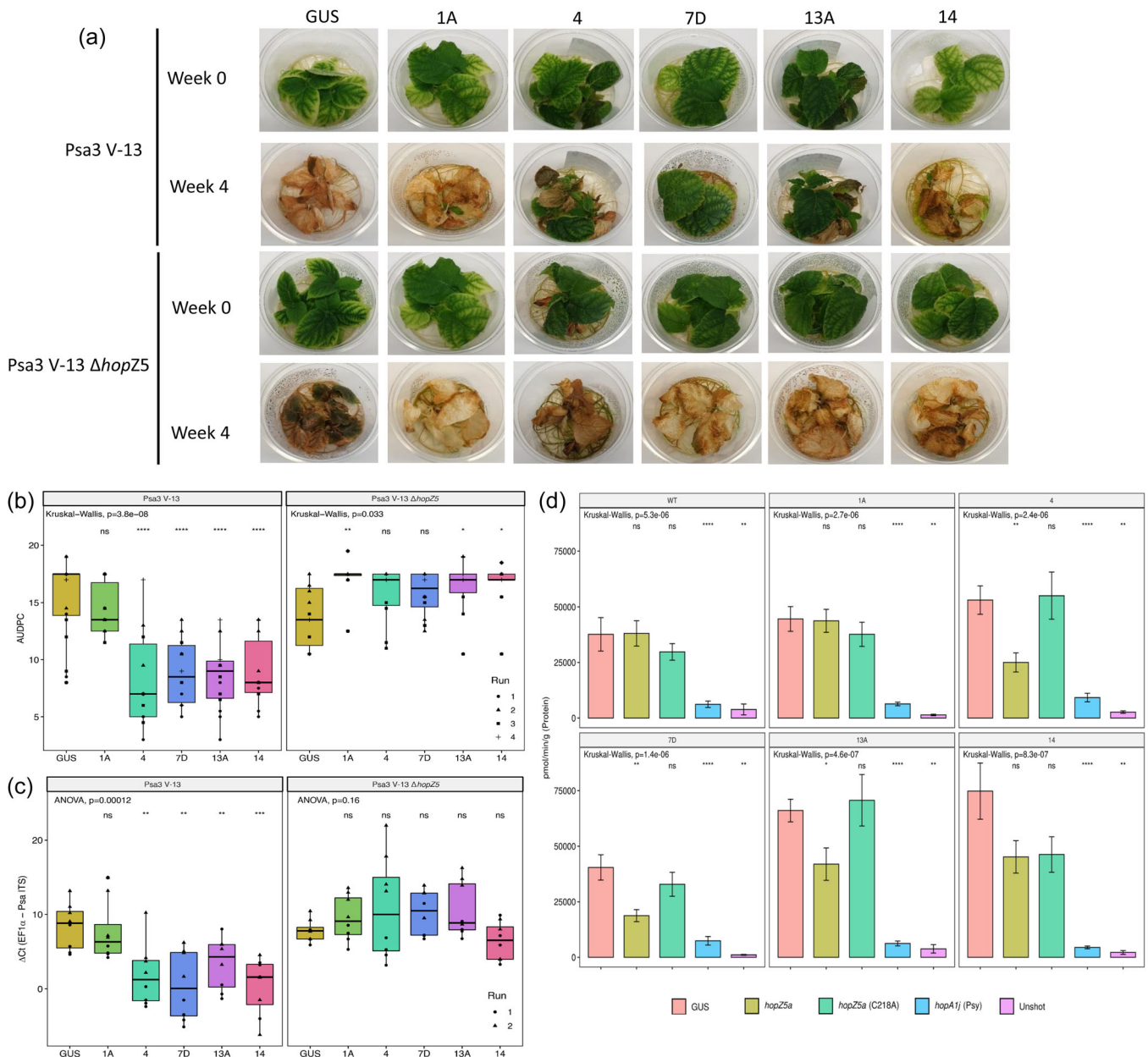

FIGURE 5 (See caption on next page).

The enzymatically inactivated HopZ5^{C218A} was used as negative control and HopA1j from *P. syringae* pv. *syringae* 61 was used as positive control (Jayaraman et al., 2021). HopZ5 appeared to trigger some ion leakage in the four moderate-to-high expressing lines (4, 7D, 13A, and 14) compared with the GUS control and low-expressing Line 1A plantlets. Taken together, these results indicate that HopZ5 was able to trigger a weak but detectable HR in Nb*PTR1a* transgenic plants under our experimental conditions.

3 | DISCUSSION

In this study, using an RNAi hairpin screening library we demonstrated that NbPTR1a recognised Psa3 effector HopZ5 in *N. benthamiana*. Furthermore, we identified that no functional kiwifruit *PTR1* orthologues capable of recognising HopZ5 are present in Psa3-susceptible 'Hort16A' kiwifruit plants. We also showed that while RIN4 is probably involved with NbPTR1a-mediated recognition of HopZ5, this interaction is not likely to be through a stable direct interaction with NbPTR1a. This activation of NbPTR1a may be through a transient interaction model or through (or with) a third interactor protein. Finally, we transformed Nb*PTR1a* into 'Hort16A' to confer the first transgenic resistance against Psa3 introduced into a commercial kiwifruit cultivar. Overall, we present that a PTR1-like function is not present in Psa susceptible *A. chinensis* kiwifruit and required complementation by Nb*PTR1a* for resistance to Psa3.

Previously, two nucleotide-binding leucine-rich repeat proteins (NLR) in *N. benthamiana* were identified using an NbNLR VIGS screening library as responsible for mediating HopZ5 recognition: *PTR1* and *ZAR1* (the latter with the assistance of *JIM2*) in Nb-0, and only *PTR1* in Nb-1 plants (Ahn et al., 2023; Schultink et al., 2019).

From our RNAi hairpin library screening, we identified a role only for *PTR1* and not for *ZAR1* in the recognition of HopZ5 in *N. benthamiana* in a manner suggesting our system relied on Nb-1 plants. Two silencing fragments, m16 and u38, both corresponding to NbZAR1, were unable to reduce HopZ5-triggered HR in *N. benthamiana* (Figure S2). While the possibility remains that the two NbZAR1-targeting fragments could not fully silence some residual NbZAR1 activity, it is clear that silencing NbPTR1 alone was sufficient to eliminate HopZ5-triggered HR in our Nb-1-like system. Meanwhile, Zheng et al. (2022) found that HopZ5 triggered HR in wild-type *N. benthamiana* but not in the *zar1* mutant, without PTR1 involvement. Although a reason for this discrepancy has not been confirmed here, *N. benthamiana* plants used for *Agrobacterium*-mediated transient expression by Ahn et al. (NbPTR1 and NbZAR1) and Zheng et al. (NbZAR1 only) are likely to be genetically different from those used in our study (NbPTR1 only), reflecting polymorphisms in NLR systems seen in naturally occurring plant populations (Barragan & Weigel, 2021; Stam et al., 2016; Van de Weyer et al., 2019).

The mechanisms of several plant NLR proteins in model plant species that recognize HopZ5 have been studied. In *Arabidopsis*, RPM1, responsible for Pto DC3000-delivered HopZ5-triggered immunity, is activated by the acetylation of RIN4 by HopZ5 (Choi et al., 2021). ZAR1 orthologues from *A. thaliana* and *N. benthamiana* recognise HopZ5 by interacting with ZED1 and JIM2, respectively (Ahn et al., 2023; Choi et al., 2021). While the mechanisms of AtRPM1-, AtZAR1- and NbZAR1-mediated recognition of HopZ5 are clear, little is known about the mechanism for NbPTR1-mediated recognition of HopZ5. SlPTR1 from *Solanum lycopersicoides* is required for recognition of AvrRpt2 and RipBN effectors when co-expressed with SlRIN4-3, which also supressed SlPTR1 autoimmunity in *N. glutinosa* transient expression experiments (Mazo-Molina et al., 2020). This accumulated evidence

FIGURE 5 PTR1a-triggered bacterial growth restriction *in planta* is HopZ5-specific. (a) Disease phenotyping of Nb*PTR1a* transgenic plantlets inoculated with Psa3 V-13 or Psa3 V-13 Δ*hopZ5*. Plantlets were flood-inoculated with Psa3 V-13 or Psa3 V-13 Δ*hopZ5* at approximately 10^6 CFU/mL. Representative photographs of plantlets were taken at 0 and 4 weeks postinoculation. (b) Quantitative analysis of disease phenotypes in (a). Individual plantlets were scored weekly on a scale of 0 (asymptomatic) to 4 (dead) for 6 weeks postinfection (dpi). Disease phenotypes were quantified by measuring the area under the disease progression curve (AUDPC). Asterisks indicate results of a Kruskal–Wallis analysis of variance and a two-tailed Welch's post hoc *t*-test between the selected transgenic lines and transgenic GUS control; *$p < 0.05$, **$p < 0.01$, ***$p < 0.001$, ****$p < 0.0001$, and ns, nonsignificant. Data were collected across four independent experimental runs. (c) Bacterial growth in Nb*PTR1a* transgenic plantlets determined by PDQeX-qPCR. Psa3 V-13 or Psa3 V-13 Δ*hopZ5* was flood-inoculated as described in (a), and bacterial presence in leaf samples was quantified at 10 days postinoculation by PDQeX DNA extraction and qPCR for the Psa3 intergenic transcribed spacer (*ITS*) region normalized to Ac*EF1α*. Error bars represent standard error of the mean from four biological replicates. Asterisks indicate results of a one-way analysis of variance (ANOVA) and a two-tailed Welch's post hoc *t*-test between the selected transgenic lines and transgenic GUS control line; *$p < 0.05$, **$p < 0.01$, ***$p < 0.001$, ****$p < 0.0001$, and ns, nonsignificant. Data from two independent experimental runs are displayed. (c) Nb*PTR1a* kiwifruit transgenic *Actinidia chinensis var. chinensis* 'Hort16A' plantlets were flood inoculated with either Psa3 V-13 or Psa3 V-13 Δ*hopZ5* at approximately 10^6 CFU/mL. Symptom development on representative pottles of Nb*PTR1a* kiwifruit transgenic plantlets was photographed before the pathogen infection and 4 weeks postinfection. β-glucuronidase (GUS) transgenic lines were used as negative controls. (d) HopZ5 triggers immunity in Nb*PTR1a* transgenic plants. HopZ5-triggered HR was monitored using a reporter eclipse assay. Effector constructs tagged with GFP, or empty vector, were coexpressed with a GUS reporter construct using biolistic bombardment in leaves from five Nb*PTR1a* transgenic lines or wild-type Hort16A. GUS activity was measured 48 h after DNA bombardment. Error bars represent the standard errors of the means for three independent biological replicates with six technical replicates each (*n* = 18). HopA1j from *Pseudomonas syringae* pv. *syringae* 61 was used as positive control and un-infiltrated leaf tissue (Unshot) as a negative control. Asterisks indicate results of a Kruskal–Wallis analysis of variance and a Wilcoxon post hoc test between the selected effector treatments and empty vector (GUS) alone; *$p < 0.05$, **$p < 0.01$, ***$p < 0.001$, ****$p < 0.0001$, and ns, nonsignificant. Data were collected across three independent experimental runs. [Color figure can be viewed at wileyonlinelibrary.com]

suggested that NbPTR1-mediated recognition of HopZ5 might be related to RIN4.

co-IP experiments showed that NbPTR1a stably interacted with NbRIN4-1 and AcRIN4-2. This RIN4 interaction with PTR1 may be necessary for activation of resistance, but does not preclude an interaction or process involving another RIN4/PTR1 interacting partner, such as Exo70 (Tsakiri et al., 2022). AcRIN4-2 is also targeted by HopZ5 (Jayaraman et al., 2023). However, a three-way HopZ5:AcRIN4-2:NbPTR1a complex was not detected in our experiments. This surprising result could be explained in two ways: the interaction between NbPTR1a and HopZ5 (particularly due to HopZ5 activity) may be too transient, or effector action may consistently interfere with the interaction, leading to immunity. Due to the disruption of the NbPTR1a-AcRIN4-2 interaction observed in the absence of a enzymatically functional HopZ5, the latter hypothesis is plausible. Nevertheless, using modelling and confirmation by yeast two-hybrid assays to assess direct interactions between NbRIN4s or AcRIN4s and NbPTR1a did not reveal an authentic interaction between these two components of resistance (Table S1 and Figure S4). There are two alternative possible explanations for these findings: (1) AlphaFold multimer is not able to predict interaction of protein pairs that include a significantly disordered partner such as RIN4, possibly as a result of the much larger structural space that needs to be explored due to the ensemble of structures predicted for disordered proteins (Uversky & Dunker, 2010) or (2) a key third protein partner, that either acts as an intermediary or as a partner that refolds critical parts of RIN4 that then enables a stable and direct interaction with NbPTR1a, is missing in the system. The first alternative, while possible for our in silico modelling, is not likely to be an explanation for the lack of interaction in the yeast two-hybrid assays as disordered protein RIN4 interactions have been reported previously (Liu et al., 2009; Redditt et al., 2019). If the second explanation of a missing third protein is correct, it suggests also that the well-known AtRIN4-AtRPM1 and AtRIN4-AtRPS2 systems may similarly still be missing key interacting protein partners, despite the intense research scrutiny that these interactions have been subjected to in previous studies. Of note was the lack of a direct interaction between HopZ5 and AcRIN4s (Figure S4). This likely suggests further evidence of either a transient interaction or an indirect mechanism of HopZ5 function. Jayaraman et al. (2023) found that four out of five key redundant Psa3 effectors collectively essential for full Psa3 virulence probably targeted host RIN4 proteins (HopZ5a, AvrPto1b, AvrRpm1a and HopF1e). Since only HopZ5 appears to be responsible for NbPTR1a-conferred immunity against Psa3, this may be further evidence that RIN4 itself may in fact not be the host protein directly guarded by PTR1a as this NLR only detects HopZ5 presence and not the other RIN4-binding effectors from Psa3. Identifying other HopZ5 plant targets in kiwifruit or N. benthamiana may reveal this authentic PTR1 guardee in the future.

Introducing NbPTR1a into kiwifruit facilitated recognition of HopZ5 and conferred resistance to Psa3 infection in susceptible 'Hort16A' plants. Among the five selected NbPTR1a transgenic lines, the strength of Psa3 resistance may not be proportional to the NbPTR1a gene expression level, but require a certain minimum threshold expression level to facilitate Psa3 resistance. The very low-expressing transgenic Line 1A, like the GUS control plants, was not able to recognise HopZ5. The other four moderate-to-high NbPTR1a expressing transgenic lines (4, 7D, 13A, and 14) showed similar levels of Psa3 resistance from disease phenotyping analysis, in planta bacterial growth quantification, or biolistic transformation reporter eclipse assays (Figures 4 and 5). Psa3 resistance in NbPTR1a transgenic kiwifruit is stably maintained from young tissue-cultured plantlets through to mature glasshouse-grown plants. Unlike NbPTR1a transgenic kiwifruit, introducing AtRPM1 into kiwifruit did not improve resistance against Psa3 infection (Table S2). Choi et al. (2021) demonstrated that AtRPM1-mediated HopZ5 recognition in Arabidopsis requires alteration of residue T166 in RIN4. It is possible that this recognition relies on co-evolved guardee and resistance proteins and the key modification may thus be restricted to Arabidopsis alleles of RIN4. Perhaps cotransforming AtRIN4 with AtRPM1 into kiwifruit may facilitate the recognition of HopZ5 to improve Psa3 resistance in the AtRPM1 transgenic plants. Alternatively, an RPM1-like function may already exist in 'Hort16A' but is somehow overcome by the effector complement present in Psa3 in a manner that does not affect NbPTR1a signalling. As AtRPM1 guards RIN4, such a suppression would constitute further evidence that RIN4 modifications may not be directly responsible for NbPTR1a signalling. Evidence for this lies in recognition of AvrRpm1$_{Pma}$ in 'Hort16A' plants when delivered by biolistic assay or Pseudomonas fluorescens (T3S), but not bacterial growth assay of Psa3 carrying AvrRpm1$_{Pma}$ (Jayaraman et al., 2021).

We show that PTR1a recognition of Psa3 is HopZ5-specific in the kiwifruit transgenic plants. HopZ5 is able to trigger a weak HR in these NbPTR1a transgenic plants (Figure S7), but only in isolation from other Psa3 effectors (Figure S6), similar to previous observations in Psa3-resistant Actinidia arguta AA07_03 (Hemara et al., 2022). It will be interesting to study whether a PTR1 homolog exists in A. arguta and can confer resistance to Psa3. The lack of ion leakage in response to HopZ5 recognition in both Actinidia species when delivered by Psa3 is unexpected, and the direct molecular mechanism underlying the NbPTR1a-mediated recognition of HopZ5 remains unclear.

We have discussed previously how breeding durable resistance genes into targeted kiwifruit cultivars will play an important role in long-term management of Psa (Hemara et al., 2022). The introduction of a functional PTR1 gene in kiwifruit through crosses with resistant plant lines carrying a functional kiwifruit orthologue of PTR1 will allow it to be efficiently tracked as it is backcrossed into various breeding lines. However, traditional plant breeding can be time-consuming and slow the development of new varieties (Kim & Kim, 2019). Alternatively, the new method of CRISPR/Cas-based 'Prime editing' has been widely applied in precision plant breeding era (Kim & Kim, 2019). Recently, this GE technology has been used in kiwifruit by deleting flowering regulation genes to reduce plant dormancy (Herath et al., 2022). Such a strategy, but with a lighter-touch editing approach, might be possible to 'repair' any

nonfunctional PTR1 orthologues present in kiwifruit but will likely require a detailed molecular understanding of the basis of the interaction between PTR1 and its associated signalling complex. This would potentially be a more efficient way to introduce resistance genes without the linkage drag caused by undesirable traits in more classical breeding approaches used to develop Psa-resistant kiwifruit varieties.

4 | MATERIALS AND METHODS

4.1 | Bacterial strains

Agrobacterium tumefaciens strain GV3101 was used for *Agrobacterium*-mediated transient assay (agroinfiltration) in *N. benthamiana*, and *A. tumefaciens* strain EHA105 was used for kiwifruit transformation (Wang et al., 2007). *Agrobacterium* strains were grown on lysogeny broth (LB) with appropriate antibiotics at 28°C. *Escherichia coli* DH5α was used for plasmid maintenance and grown in LB medium at 37°C. All strains were stored in 20% glycerol + LB at −80°C.

Knockout strains of *P. syringae* pv. *actinidiae* ICMP 18884 biovar 3 (Psa3 V-13) Δ*hrcC* and Δ*hopZ5* were previously generated through transposon mutagenesis and homologous recombination, respectively (Colombi et al., 2017; Hemara et al., 2022). The Psa3 Δ*hrcC* strain contains all Psa3 effectors but without a functional type III secretion system to delivery effector proteins into a host plant (Jayaraman et al., 2021). Bacteria were streaked from glycerol stocks onto LB agar supplemented with 12.5 µg/mL nitrofurantoin and 40 µg/mL cephalexin (Sigma-Aldrich).

4.2 | Cloning and gene synthesis

Nb*PTR1* genes were identified by BLAST from *N. benthamiana* (version 0.4.4) (Bombarely et al., 2012) and PCR products were amplified from *N. benthamiana* genomic DNA. Kiwifruit *PTR1* candidate homologues were identified by BLAST from the *A. chinensis* var. *chinensis* 'Red5' genome (Pilkington et al., 2018). Kiwifruit *PTR1* candidate homologues were PCR amplified from *A. chinensis* var. *chinensis* 'Hort16A' genomic DNA. Sequences of all the primers are provided in Table S3.

PCR products of candidate genes were purified using the Zymoclean Gel DNA Recovery kit (Zymo Research) and then cloned into pENTR/D/SD entry vector using the In-Fusion cloning kit (Takara). Inserts of all plasmids were sequenced by Macrogen, Korea. The silencing fragment amplified from hairpin constructs were cloned in the pTKO2 hairpin vector (Brendolise et al., 2017). The glycosyltransferases gene, *F3GGT1 (GGT)*, from red-fleshed kiwifruit (*A. chinensis*) (Montefiori et al., 2011) was used as the control fragment for hairpin silencing fragments and the pENTR-GGT entry clone was recombined by Gateway cloning into pTKO$_2$ (Brendolise et al., 2017) to generate the pTKO$_2$-GGT control vector. The full-length candidates were cloned in the pHEX2 vector using Gateway

cloning (Thermo Fisher Scientific), respectively. Similarly, the control vector pHEX2-GUS was constructed by Gateway LR reaction of the pENTR-GUS (Invitrogen) into the pHEX2 vector (Hellens et al., 2005). The effector HopZ5 was cloned into a binary vector (pICH86988) under the control of a 35SCaMV promoter (Jayaraman et al., 2017).

The nucleotide sequence of synthetic Nb*PTR1* (NbPTR1$_{syn}$) was designed using the GenSmart™ Codon Optimization tool (https://www.genscript.com/tools/gensmart-codon-optimization) with manual editing (Figure S2). NbPTR1$_{syn}$ was synthesized by GenScript (Singapore) and cloned into the pHEX2 vector using Gateway cloning (Thermo Fisher Scientific).

For the yeast two-hybrid assay, the full-length NbPTR1a and RIN4s orthologous were firstly cloned in the pHEX2 vector and recombined into pDEST32 (pBDGAL4, bait) and pDEST22(pADGAL4, prey; Invitrogen) using Gateway cloning (Thermo Fisher Scientific), respectively. Similarly, the effector HopZ5 was firstly cloned in the pART8 vector and recombined into pDEST32 vector using Gateway cloning (Thermo Fisher Scientific). Bait and prey constructs were transformed into *Saccharomyces cerevisiae* strains PJ69-4α (bait) and PJ69-4a (prey), respectively (James et al., 1996).

4.3 | RNA/DNA extraction and qPCR

Genomic DNA from *A. chinensis* var. *chinensis* 'Hort16A', *A. thaliana* Col-0, or *N. benthamiana* leaf was extracted using the DNeasy Plant Mini Kit (Qiagen), following the manufacturer's instructions. RNA from young kiwifruit tissue culture leaves was extracted using the Spectrum Plant Total RNA kit (Sigma-Aldrich), following the manufacturer's protocol except the incubation temperature of lysed tissue sample was increased to 65°C.

To check the expression of Nb*PTR1a* in transgenic plants, complementary DNA was synthesised using extracted RNA as the template and the QuantiTect Reverse Transcription kit (Qiagen) by following the manufacturer's instructions. qPCR was performed with specific primers (Table S3) and LightCycler 480 SYBR Green I Mastermix (Roche) using the LightCycler 480 II real-time PCR device (Roche). Each reaction volume was 10 µL and reactions were run in quadruplicate, including nontemplate negative controls. qPCR followed a three-step reaction of 95°C for 10 s, 60°C for 10 s and 72°C for 20 s for 50 cycles. The data were analysed by the LightCycler 480 software 1.5 using the target/reference ratio to compare the target gene expression level to that of the reference gene, AcEF1α. Sequences of all primers are provided in Table S3.

4.4 | Plant materials and growth condition

For transient expression experiments, *N. benthamiana* plants were grown in a temperature-controlled glasshouse at 22°C to 24°C under long-day conditions (16 h light, 8 h dark).

Tissue-cultured *A. chinensis* var. *chinensis* 'Hort16A' plantlets were purchased from Multiflora Laboratories (New Zealand).

Plantlets were grown on supplied Murashige and Skoog (MS) agar (M1, Table S4) in 400 mL-lidded plastic tubs. Plantlets were grown in a tissue culture room at 20°C under long-day conditions (16 h light, 8 h dark) with cool white fluorescent light (~120 µmol^{-2} m s^{-1}). For glasshouse experiments, tissue culture plantlets were transferred to soil and grown for at least 3 months before testing. Rooted kiwifruit plants grown in the soil were fertilized with commercial WUXAL (2 mL/L) every 2 weeks.

4.5 | Transient overexpression and RNAi library screen in *Nicotiana benthamiana*

Transient expression and the RNAi library screen in *N. benthamiana* were performed as previously described (Brendolise et al., 2017). In brief, freshly grown *A. tumefaciens* culture containing either RNAi hairpin constructs or pTKO2_GGT control vector was re-suspended in infiltration buffer (10 mM MgCl$_2$, 100 µM acetosyringone). The cells were diluted to the appropriate concentrations and infiltrated in leaves of 3-week-old plants using a needleless syringe and the infiltrated area was marked. After 48-h infiltration, the marked infiltrated area were inoculated with the HopZ5 construct or the GUS control. Photographs were taken 4–5 days after HopZ5 infiltration.

4.6 | Electrolyte leakage quantification in *N. benthamiana*

Electrolyte leakage experiments in *N. benthamiana* were performed as previously described (Ahn et al., 2023). In brief, six leaf disks (6 mm) from the agroinfiltrated patches were collected 2 days after the last infiltration and washed in distilled water for 30 min. Leaf discs were placed in 2 mL of sterile water and the conductivity was measured over 26 h by using a LAQUAtwin EC-33 conductivity meter (Horiba). HopZ5 was used as the positive control and infiltration buffer (10 mM MgCl$_2$, 100 µM acetosyringone) as a negative control. The standard errors of the means were calculated from five biological replicates. Data were collected across two independent experimental runs and data from both runs were plotted (*n* = 10).

4.7 | Transient expression in *N. benthamiana* and co-IP

The transient expression in *N. benthamiana* and co-immunoprecipitation assay was described previously (Hemara et al., 2022). Briefly, *A. tumefaciens* AGL1 (YFP-tagged effectors; Choi et al., 2017) or GV3101 pMP90 (FLAG-tagged AcRIN4s; Yoon & Rikkerink, 2020) was freshly grown in LB with appropriate antibiotics at 28°C with shaking at 200 rpm. Cells were pelleted by centrifugation at 4000g for 10 min and resuspended in infiltration buffer (10 mM MgCl$_2$, 5 mM EGTA, 100 µM acetosyringone). Cell suspensions were diluted to a final OD$_{600}$ of 0.1 and infiltrated into at least

two fully expanded leaves of 4- to 5-week-old *N. benthamiana* plants using a needleless syringe. All *Agrobacterium*-mediated transformation experiments were performed using pre-mixed *Agrobacterium* cultures for the stipulated effector-RIN4 combinations in a single injection for co-immunoprecipitation experiments (see below). YFP was used as a negative control for effectors. Tissues (0.5 g per sample) were collected 2 days postinfiltration and ground to a homogeneous powder in liquid nitrogen and resuspended in 1 mL of protein extraction buffer (1× PBS, 1% *n*-dodecyl β-D-maltoside or DDM (Invitrogen), and 0.1 tablet cOmplete™ protease inhibitor cocktail (Sigma-Aldrich) in NativePAGE™ buffer (Invitrogen). Extracted protein samples were centrifuged at 20,000g for 2 min at 4°C and the supernatant was collected for immunoprecipitation using the Pierce™ Anti-c-Myc Magnetic Beads (88843; Thermo-Fisher Scientific) according to the manufacturer's instructions. Total and immunoprecipitated proteins were resolved on a 4%–12% sodium dodecyl sulfate–polyacrylamide gel electrophoresis gel. Western blots using polyvinylidene difluoride membranes were prepared and probed using horseradish peroxidase (HRP)-conjugated antibodies in 0.2% I-Block (Invitrogen). Detection was achieved using the Clarity™ MAX Western ECL Substrate (Bio-Rad). The antibodies used were α-FLAG-HRP (A8592; Sigma-Aldrich), α-GFP-HRP (A10260; Thermo-Fisher Scientific), and α-Myc-HRP (SAB4200742; Sigma-Aldrich).

4.8 | Kiwifruit transformation

A. tumefaciens-mediated transformation of *A. chinensis* was performed as previously described (Wang et al., 2007). The medium used for kiwifruit transformation in this study was adapted from Wang et al. (2007) (Table S4). Briefly, leaf strips excised from in vitro-grown shoots were inoculated with suspension culture of *Agrobacterium* strain EHA105 (at OD ~0.8–1.0) with infection buffer (M2) for 45 min. Inoculated leaf strips were transferred to cocultivation medium (M3) and incubated at 24°C for 2 days. After cocultivation, the leaf strips were transferred to regeneration and selection medium containing kanamycin 150 mg/L (M4). Individual calli were excised from the leaf strips for further selection and bud induction, and adventitious buds regenerated from the calli were excised and transferred to shoot elongation medium (M5). When shoots had grown to 1–2 cm high, they were transplanted onto rooting medium (M6).

4.9 | In planta bacterial growth quantification assays

Resistance to Psa was determined by flooding tissue culture-grown plantlets or leaf-dip for glass house-grown plants with Psa inoculum diluted to 10^7 cfu/mL in 10 mM MgCl$_2$ supplemented with 0.025% Silwet™ L-77 surfactant (PhytoTechnology Laboratories®). Tissue culture plantlets were flooded for 3 min each. For glasshouse plants, leaves were submerged in inoculum for 20 s. Leaves were sampled in

quadruplicate at selected time points using a using a 1-cm^2 cork borer with each replicate carrying four leaf discs, ground in 10 mM MgSO$_4$ using a Storm24 Bullet Blender (Next Advance). For tissue culture experiments, Psa growth was quantified by plating a 10-fold dilution series onto LB agar. Samples were incubated for 2 days before colony counting to calculate cfu/mL.

For both tissue culture and glasshouse experiments, Psa was also quantified using a qPCR method adapted from that of Hemara et al. (2022). Briefly, genomic DNA was extracted from leaf samples using the PDQeX nucleic acid extractor (MicroGEM). Real-time qPCR was carried out on an Illumina Eco real-time PCR platform using SsoFast EvaGreen Supermix (BioRad). qPCR was performed using Psa intergenic transcribed spacer (*ITS*) and plant *AcEF1α* primers (Table S3). Relative Psa biomass was calculated by normalising the cycle threshold (C_t) values for Psa *ITS* to those of the kiwifruit *AcEF1α* reference gene and plotting the C_t difference for each sample. Results were plotted in R using the ggplot2 and ggpubr packages, with significance values calculated using a two-tailed Welch's post hoc *t*-test.

4.10 | Disease phenotyping assays

Plantlets were flood-inoculated with Psa inoculum at approximately 10^6 cfu/mL. Individual plantlets were scored weekly on a scale of 0 (asymptomatic) to 4 (dead) for 6 weeks dpi. Disease phenotypes were quantified using an area under the disease progression curve (AUDPC) adapted from previous work (Schandry, 2017). Briefly, mean disease index (DI) scores were plotted for Weeks 2–6. AUDPC values were calculated for each sample and fitted to a linear mixed effects model using the lme4 package (Bates et al., 2015). Post hoc Tukey's tests were performed via multcomp package (Hothorn et al., 2008). All statistical analyses were conducted in R, with figures produced using the ggplot2 package (R Core Team, 2022; Wickham, 2016).

4.11 | Biolistic cobombardment reporter eclipse assay

The biolistic report eclipse assay was described previously (Jayaraman et al., 2021). Six bombardments were performed for each effector in an experiment, and carried out in triplicate (technical replicates) and expressed in terms of pmol of MU produced per minute per gram of total protein. The means and standard errors were calculated from the six replicates conducted per experiment, from three independent experimental runs (*n* = 18). Data for each treatment were stacked from all three runs and were analysed by ANOVA followed by a Tukey's HSD post hoc test.

4.12 | Phylogenetic analyses

The sequence information of NbNRG1 (GenBank: DQ054580.1), AtRPS2 (GenBank: AF487807.1), AtRPM1 (GenBank: KC211321.1),

MdMr5 (GenBank: KT013245.1), SlPtr1 (GenBank: MT134103.1), GmRPG1r (GenBank: KF958751.1), GmRPG1b (GenBank: AY452685.1), AtZAR1 (GenBank: AK227017.1) and NbZAR1 (GenBank: MH532570.1) were obtained from NCBI. The top four BLASTP hits of each AcPTR1 orthologues NB-ARC domains with at least 20% identical residues in the domain were identified in the *N. benthamiana* (version 0.4.4) genome sequence (Bombarely et al., 2012). In the phylogenetic tree, the NB-ARC domain of each protein hit was determined using Interpro scan (https://www.ebi.ac.uk/interpro/), and the nucleotide sequences of the NB-ARC domain for each contracts were aligned to check for the presence of the NB-ARC conserved motifs. Multiple nucleotide sequence alignment were created by using MUSCLE alignment in Geneious Prime. The nucleotide distance was calculated by GAMMA GTR model with the algorithm of rapid bootstrapping and search for best-scoring ML tree and phylogenetic trees were generated using RAxML method (Stamatakis, 2014) with 100 bootstrap replicates in Geneious Prime.

CONFLICT OF INTEREST STATEMENT

The authors declare no conflict of interest.

DATA AVAILABILITY STATEMENT

All the relevant data are provided in this article and its supplementary information. All the materials supporting the findings of this study are available from the corresponding authors upon request.

ORCID

Shin-Mei Yeh https://orcid.org/0009-0008-3068-1173
Minsoo Yoon https://orcid.org/0000-0001-5524-3972
Lauren M. Hemara https://orcid.org/0000-0003-0316-3545
Ronan K. Y. Chen https://orcid.org/0000-0002-2471-4628
Tianchi Wang http://orcid.org/0000-0003-1635-7146
Kerry Templeton http://orcid.org/0000-0001-8047-2638
Erik H. A. Rikkerink https://orcid.org/0000-0003-4682-5078
Jay Jayaraman http://orcid.org/0000-0003-4959-9467
Cyril Brendolise http://orcid.org/0000-0001-8213-8094

REFERENCES

Ahn, Y.J., Kim, H., Choi, S., Mazo-Molina, C., Prokchorchik, M., Zhang, N. et al. (2023) Ptr1 and ZAR1 immune receptors confer overlapping and distinct bacterial pathogen effector specificities. *New Phytologist*, 239, nph.19073. Available from: https://doi.org/10.1111/nph.19073

Alfano, J.R., Charkowski, A.O., Deng, W.-L., Badel, J.L., Petnicki-Ocwieja, T., van Dijk, K. et al. (2000) The *Pseudomonas syringae* Hrp pathogenicity island has a tripartite mosaic structure composed of a cluster of type III secretion genes bounded by exchangeable effector and conserved effector loci that contribute to parasitic fitness and pathogenicity in plants. *Proceedings of the National Academy of Sciences of the United States of America*, 97, 4856–4861. Available from: https://doi.org/10.1073/pnas.97.9.4856

Axtell, M.J. & Staskawicz, B.J. (2003) Initiation of RPS2-specified disease resistance in *Arabidopsis* is coupled to the AvrRpt2-directed elimination of RIN4. *Cell*, 112, 369–377. Available from: https://doi.org/10.1016/S0092-8674(03)00036-9

Barragan, A.C. & Weigel, D. (2021) Plant NLR diversity: the known unknowns of pan-NLRomes. *The Plant Cell*, 33, 814–831. Available from: https://doi.org/10.1093/plcell/koaa002

Bates, D., Mächler, M., Bolker, B. & Walker, S. (2015) Fitting linear mixed-effects models using lme4. *Journal of Statistical Software*, 67, 1–48. Available from: https://doi.org/10.18637/jss.v067.i01

Block, A., Li, G., Fu, Z.Q. & Alfano, J.R. (2008) Phytopathogen type III effector weaponry and their plant targets. *Current Opinion in Plant Biology*, 11, 396–403. Available from: https://doi.org/10.1016/j.pbi.2008.06.007

Bombarely, A., Rosli, H.G., Vrebalov, J., Moffett, P., Mueller, L.A. & Martin, G.B. (2012) A draft genome sequence of *Nicotiana benthamiana* to enhance molecular plant-microbe biology research. *Molecular Plant-Microbe Interactions*®, 25, 1523–1530. Available from: https://doi.org/10.1094/MPMI-06-12-0148-TA

Brendolise, C., Martinez-Sanchez, M., Morel, A., Chen, R., Dinis, R., Deroles, S. et al. (2018) NRG1-mediated recognition of HopQ1 reveals a link between PAMP- and effector-triggered immunity (preprint). *bioRxiv*. In press. Available from: https://doi.org/10.1101/293050

Brendolise, C., Montefiori, M., Dinis, R., Peeters, N., Storey, R.D. & Rikkerink, E.H. (2017) A novel hairpin library-based approach to identify NBS–LRR genes required for effector-triggered hypersensitive response in *Nicotiana benthamiana*. *Plant Methods*, 13, 32. Available from: https://doi.org/10.1186/s13007-017-0181-7

Choi, S., Jayaraman, J., Segonzac, C., Park, H.-J., Park, H., Han, S.-W. et al. (2017) *Pseudomonas syringae pv. actinidiae* type III effectors localized at multiple cellular compartments activate or suppress innate immune responses in *Nicotiana benthamiana*. *Frontiers in Plant Science*, 8, 2157. Available from: https://doi.org/10.3389/fpls.2017.02157

Choi, S., Prokchorchik, M., Lee, H., Gupta, R., Lee, Y., Chung, E.-H. et al. (2021) Direct acetylation of a conserved threonine of RIN4 by the bacterial effector HopZ5 or AvrBsT activates RPM1-dependent immunity in *Arabidopsis*. *Molecular Plant*, 14, 1951–1960. Available from: https://doi.org/10.1016/j.molp.2021.07.017

Colombi, E., Straub, C., Künzel, S., Templeton, M.D., McCann, H.C. & Rainey, P.B. (2017) Evolution of copper resistance in the kiwifruit pathogen *Pseudomonas syringae pv. actinidiae* through acquisition of integrative conjugative elements and plasmids. *Environmental Microbiology*, 19, 819–832. Available from: https://doi.org/10.1111/1462-2920.13662

Cui, H., Tsuda, K. & Parker, J.E. (2015) Effector-triggered immunity: from pathogen perception to robust defense. *Annual Review of Plant Biology*, 66, 487–511. Available from: https://doi.org/10.1146/annurev-arplant-050213-040012

Dangl, J.L. & Jones, J.D.G. (2001) Plant pathogens and integrated defence responses to infection. *Nature*, 411, 826–833. Available from: https://doi.org/10.1038/35081161

Fahrentrapp, J., Broggini, G.A.L., Kellerhals, M., Peil, A., Richter, K., Zini, E. et al. (2013) A candidate gene for fire blight resistance in Malus × robusta 5 is coding for a CC–NBS–LRR. *Tree Genetics & Genomes*, 9, 237–251. Available from: https://doi.org/10.1007/s11295-012-0550-3

Hellens, R.P., Allan, A.C., Friel, E.N., Bolitho, K., Grafton, K., Templeton, M.D. et al. (2005) Transient expression vectors for functional genomics, quantification of promoter activity and RNA silencing in plants. *Plant Methods*, 1, 13. Available from: https://doi.org/10.1186/1746-4811-1-13

Hemara, L.M., Jayaraman, J., Sutherland, P.W., Montefiori, M., Arshed, S., Chatterjee, A. et al. (2022) Effector loss drives adaptation of *Pseudomonas syringae pv. actinidiae* biovar 3 to *Actinidia arguta*. *PLoS Pathogens*, 18, e1010542. Available from: https://doi.org/10.1371/journal.ppat.1010542

Herath, D., Voogd, C., Mayo-Smith, M., Yang, B., Allan, A.C., Putterill, J. et al. (2022) CRISPR-Cas9 -mediated mutagenesis of kiwifruit *BFT* genes results in an evergrowing but not early flowering phenotype. *Plant Biotechnology Journal*, 20, 2064–2076. Available from: https://doi.org/10.1111/pbi.13888

Hothorn, T., Bretz, F. & Westfall, P. (2008) Simultaneous inference in general parametric models. *Biometrical Journal*, 50, 346–363. Available from: https://doi.org/10.1002/bimj.200810425

James, P., Halladay, J. & Craig, E.A. (1996) Genomic libraries and a host strain designed for highly efficient two-hybrid selection in yeast. *Genetics*, 144, 1425–1436. Available from: https://doi.org/10.1093/genetics/144.4.1425

Jayaraman, J., Chatterjee, A., Hunter, S., Chen, R., Stroud, E.A., Saei, H. et al. (2021) Rapid methodologies for assessing *Pseudomonas syringae pv. actinidiae* colonization and effector-mediated hypersensitive response in kiwifruit. *Molecular Plant-Microbe Interactions*®, 34, 880–890. Available from: https://doi.org/10.1094/MPMI-02-21-0043-R

Jayaraman, J., Choi, S., Prokchorchik, M., Choi, D.S., Spiandore, A., Rikkerink, E.H. et al. (2017) A bacterial acetyltransferase triggers immunity in *Arabidopsis thaliana* independent of hypersensitive response. *Scientific Reports*, 7, 3557. Available from: https://doi.org/10.1038/s41598-017-03704-x

Jayaraman, J., Yoon, M., Hemara, L.M., Bohne, D., Tahir, J., Chen, R.K.Y. et al. (2023) Contrasting effector profiles between bacterial colonisers of kiwifruit reveal redundant roles converging on PTI -suppression and RIN4. *New Phytologist*, 238, 1605–1619. Available from: https://doi.org/10.1111/nph.18848

Jones, J.D.G. & Dangl, J.L. (2006) The plant immune system. *Nature*, 444, 323–329. Available from: https://doi.org/10.1038/nature05286

Kessens, R., Ashfield, T., Kim, S.H. & Innes, R.W. (2014) Determining the GmRIN4 requirements of the soybean disease resistance proteins Rpg1b and Rpg1r using a *Nicotiana glutinosa*-based agroinfiltration system. *PLoS One*, 9, e108159. Available from: https://doi.org/10.1371/journal.pone.0108159

Kim, G.H., Jung, J.S. & Koh, Y.J. (2017) Occurrence and epidemics of bacterial canker of kiwifruit in Korea. *The Plant Pathology Journal*, 33, 351–361. Available from: https://doi.org/10.5423/PPJ.RW.01.2017.0021

Kim, H., Ahn, Y.J., Lee, H., Chung, E.-H., Segonzac, C. & Sohn, K.H. (2023) Diversified host target families mediate convergently evolved effector recognition across plant species. *Current Opinion in Plant Biology*, 74, 102398. Available from: https://doi.org/10.1016/j.pbi.2023.102398

Kim, J.-I. & Kim, J.-Y. (2019) New era of precision plant breeding using genome editing. *Plant Biotechnology Reports*, 13, 419–421. Available from: https://doi.org/10.1007/s11816-019-00581-w

Lindeberg, M., Cunnac, S. & Collmer, A. (2012) Pseudomonas syringae type III effector repertoires: last words in endless arguments. *Trends in Microbiology*, 20, 199–208. Available from: https://doi.org/10.1016/j.tim.2012.01.003

Liu, J., Elmore, J.M., Fuglsang, A.T., Palmgren, M.G., Staskawicz, B.J. & Coaker, G. (2009) RIN4 functions with plasma membrane H+-

ATPases to regulate stomatal apertures during pathogen attack. *PLoS Biology*, 7, e1000139. Available from: https://doi.org/10.1371/journal.pbio.1000139

Mackey, D., Belkhadir, Y., Alonso, J.M., Ecker, J.R. & Dangl, J.L. (2003) Arabidopsis RIN4 is a target of the type III virulence effector AvrRpt2 and modulates RPS2-mediated resistance. *Cell*, 112, 379–389. Available from: https://doi.org/10.1016/S0092-8674(03)00040-0

Mazo-Molina, C., Mainiero, S., Hind, S.R., Kraus, C.M., Vachev, M., Maviane-Macia, F. et al. (2019) The *Ptr1* locus of *Solanum lycopersicoides* confers resistance to race 1 strains of *Pseudomonas syringae* pv. *tomato* and to *Ralstonia pseudosolanacearum* by recognizing the type III effectors AvrRpt2 and RipBN. *Molecular Plant-Microbe Interactions*®, 32, 949–960. Available from: https://doi.org/10.1094/MPMI-01-19-0018-R

Mazo-Molina, C., Mainiero, S., Haefner, B.J., Bednarek, R., Zhang, J., Feder, A. et al. (2020) *Ptr1* evolved convergently with *RPS2* and *Mr5* to mediate recognition of AvrRpt2 in diverse solanaceous species. *The Plant Journal*, 103, 1433–1445. Available from: https://doi.org/10.1111/tpj.14810

McCann, H.C., Rikkerink, E.H.A., Bertels, F., Fiers, M., Lu, A., Rees-George, J. et al. (2013) Correction: genomic analysis of the Kiwifruit pathogen *Pseudomonas syringae pv. actinidiae* provides insight into the origins of an emergent plant disease. *PLoS Pathogens*, 9, e1003503. Available from: https://doi.org/10.1371/journal.ppat.1003503

Mirdita, M., Schütze, K., Moriwaki, Y., Heo, L., Ovchinnikov, S. & Steinegger, M. (2022) ColabFold: making protein folding accessible to all. *Nature Methods*, 19, 679–682. Available from: https://doi.org/10.1038/s41592-022-01488-1

Montefiori, M., Espley, R.V., Stevenson, D., Cooney, J., Datson, P.M., Saiz, A. et al. (2011) Identification and characterisation of F3GT1 and F3GGT1, two glycosyltransferases responsible for anthocyanin biosynthesis in red-fleshed kiwifruit (*Actinidia chinensis*). *The Plant Journal*, 65, 106–118. Available from: https://doi.org/10.1111/j.1365-313X.2010.04409.x

Ngou, B.P.M., Ahn, H.-K., Ding, P. & Jones, J.D.G. (2021) Mutual potentiation of plant immunity by cell-surface and intracellular receptors. *Nature*, 592, 110–115. Available from: https://doi.org/10.1038/s41586-021-03315-7

Pilkington, S.M., Crowhurst, R., Hilario, E., Nardozza, S., Fraser, L., Peng, Y. et al. (2018) A manually annotated *Actinidia chinensis* var. chinensis (kiwifruit) genome highlights the challenges associated with draft genomes and gene prediction in plants. *BMC Genomics*, 19, 257. Available from: https://doi.org/10.1186/s12864-018-4656-3

R Core Team. (2022) *R: a language and environment for statistical computing*. Vienna, Austria: R Foundation for Statistical Computing.

Redditt, T.J., Chung, E.-H., Zand Karimi, H., Rodibaugh, N., Zhang, Y. & Trinidad, J.C. et al. (2019) AvrRpm1 functions as an ADP-ribosyl transferase to modify NOI-domain containing proteins, including *Arabidopsis* and Soybean RPM1-interacting protein 4. *Plant Cell*, 31, 2664–2681. https://doi.org/10.1105/tpc.19.00020

Schandry, N. (2017) A practical guide to visualization and statistical analysis of *R. solanacearum* infection data using R. *Frontiers in Plant Science*, 8, 623.

Schultink, A., Qi, T., Bally, J. & Staskawicz, B. (2019) Using forward genetics in *Nicotiana benthamiana* to uncover the immune signaling pathway mediating recognition of the *Xanthomonas perforans* effector XopJ4. *New Phytologist*, 221, 1001–1009. Available from: https://doi.org/10.1111/nph.15411

Scortichini, M. (1994) Occurrence of *Pseudomonas syringae* pv. *actinidiae* on kiwifruit in Italy. *Plant Pathology*, 43, 1035–1038. Available from: https://doi.org/10.1111/j.1365-3059.1994.tb01654.x

Scortichini, M., Marcelletti, S., Ferrante, P., Petriccione, M. & Firrao, G. (2012) *Pseudomonas syringae* pv. *actinidiae*: a re-emerging, multi-faceted, pandemic pathogen. *Molecular Plant Pathology*, 13, 631–640. Available from: https://doi.org/10.1111/j.1364-3703.2012.00788.x

Serizawa, S., Ichikawa, T., Takikawa, Y., Tsuyumu, S. & Goto, M. (1989) Occurrence of bacterial canker of kiwifruit in Japan: description of symptoms, isolation of the pathogen and screening of bactericides. *Japanese Journal of Phytopathology*, 55, 427–436. Available from: https://doi.org/10.3186/jjphytopath.55.427

Stam, R., Scheikl, D. & Tellier, A. (2016) Pooled enrichment sequencing identifies diversity and evolutionary pressures at NLR resistance genes within a wild tomato population. *Genome Biology and Evolution*, 8, 1501–1515. Available from: https://doi.org/10.1093/gbe/evw094

Stamatakis, A. (2014) RAxML version 8: a tool for phylogenetic analysis and post-analysis of large phylogenies. *Bioinformatics*, 30, 1312–1313. Available from: https://doi.org/10.1093/bioinformatics/btu033

Thomas, W.J., Thireault, C.A., Kimbrel, J.A. & Chang, J.H. (2009) Recombineering and stable integration of the *Pseudomonas syringae* pv. *syringae* 61hrp/hrc cluster into the genome of the soil bacterium *Pseudomonas fluorescens* Pf0-1. *The Plant Journal*, 60, 919–928. Available from: https://doi.org/10.1111/j.1365-313X.2009.03998.x

Tsakiri, D., Kotsaridis, K., Marinos, S., Michalopoulou, V.A., Kokkinidis, M. & Sarris, P.F. (2022) The core effector RipE1 of *Ralstonia solanacearum* interacts with and cleaves Exo70B1 and is recognized by the Ptr1 immune receptor (preprint). *bioRxiv*. In press. Available from: https://doi.org/10.1101/2022.08.31.506019

Uversky, V.N. & Dunker, A.K. (2010) Understanding protein non-folding. *Biochimica et Biophysica Acta (BBA) - Proteins and Proteomics*, 1804, 1231–1264. Available from: https://doi.org/10.1016/j.bbapap.2010.01.017

Vanneste, J.L. (2017) The scientific, economic, and social impacts of the New Zealand outbreak of bacterial canker of Kiwifruit (*Pseudomonas syringae* pv. *actinidiae*). *Annual Review of Phytopathology*, 55, 377–399. Available from: https://doi.org/10.1146/annurev-phyto-080516-035530

Wang, T., Atkinson, R. & Janssen, B. (2007) The choice of *Agrobacterium* strain for transformation of kiwifruit. *Acta Horticulturae*, 753, 227–232. Available from: https://doi.org/10.17660/ActaHortic.2007.753.26

Van de Weyer, A.-L., Monteiro, F., Furzer, O.J., Nishimura, M.T., Cevik, V., Witek, K. et al. (2019) A Species-Wide inventory of NLR genes and alleles in *Arabidopsis thaliana*. *Cell*, 178, 1260–1272. Available from: https://doi.org/10.1016/j.cell.2019.07.038

Wickham, H. (2016) *ggplot2: Elegant Graphics for Data Analysis*. New York: Springer-Verlag.

Yoon, M. & Rikkerink, E.H.A. (2020) *Rpa1* mediates an immune response to *avrRpm1* $_{Psa}$ and confers resistance against *Pseudomonas syringae* pv. *actinidiae*. *The Plant Journal*, 102, 688–702. Available from: https://doi.org/10.1111/tpj.14654

Zheng, X., Zhou, Z., Gong, Z., Hu, M., Ahn, Y.J., Zhang, X. et al. (2022) Two plant NLR proteins confer strain-specific resistance conditioned by an effector from *Pseudomonas syringae* pv. *actinidiae*. *Journal of Genetics and Genomics*, 49, 823–832. Available from: https://doi.org/10.1016/j.jgg.2022.06.006

SUPPORTING INFORMATION

Additional supporting information can be found online in the Supporting Information section at the end of this article.